Electronic Supplementary Information

A 3D Porous Nitrogen-Doped Carbon-Nanofiber-Supported Palladium Composite as an Efficient Catalytic Cathode for Lithium-Oxygen Batteries

Jun Wang,[a] Lili Liu,[a] Shulei Chou,[a] Huakun Liu[a] and Jiazhao Wang*[a]

[a] Institute for Superconducting and Electronic Materials (ISEM), University of Wollongong, Wollongong, NSW 2522, Australia

*Address correspondence to jiazhao@uow.edu.au

Experimental Section

Preparation of Pd/PNCNF Composites. Firstly, the PPy nanofibers were obtained via the polymerization reaction route. 720 mg cetrimonium bromide (CTAB) was dissolved in 200 mL 1 M HCl solution by constant stirring, and the solution was cooled down to 0-5 ^{o}C in an ice bath. 330 mg distilled pyrrole (Py) monomer was then added into the solution, and vigorous stirring continued for 0.5 h. Meanwhile, 1130 mg ammonium peroxydisulfate (APS) was completely dispersed in 20 mL distilled water. This solution was dropped into the Py-monomer-containing solution and allowed to react for 24 h. After that, the black precipitate (the PPy nanofibers) was suction filtered and washed several times with 1 M HCl solution and distilled water, followed by drying in a vacuum oven at 80 ^{o}C for 12 h. To prepare the carbon nanofibers with porous nitrogen-doped structure, the as-formed PPy nanofibers were mixed with KOH in a mass ratio of 1 : 2, and the mixture was heated up to 650 ^{o}C for 0.5 h at a heating rate of 3 ^{o}C min^{-1} and then cooled down to room temperature naturally under a N_2 atmosphere. The activated product was successively washed with 1 M HCl solution and distilled water until the filtrate became neutral. The PNCNFs were obtained after drying in a vacuum oven at 80 ^{o}C overnight.

The PNCNFs were added into 50 mL distilled water and ultrasonically treated for 1 h. Subsequently, $PdCl_2$ was dissolved in 10 mL, 1 M HCl solution, which was mixed with the PNCNF suspension with strong stirring for 1 h afterwards, and the pH of the above suspension was adjusted to 10 using 1 M NaOH solution. Icy cold aqueous 0.15 M $NaBH_4$ was added dropwise into the precursor solution, and it was further stirred for 12 h. After the reaction, the precipitate was washed with distilled water and ethanol, and then dried in a vacuum oven at 80 ^{o}C for 12 h. By using this method, three Pd/PNCNF composites were fabricated using 0.1, 0.2, and 0.3 mmol $PdCl_2$ precursor with the same amount of PNCNFs (50 mg). The amounts of $NaBH_4$ solution serving as reduction agent were 10, 30, and 45 mL, and the resulting samples were designated as Pd/PNCNF-1, Pd/PNCNF-2, and Pd/PNCNF-3, respectively. The pure Pd particles used in the characterization for reference were prepared by the same method without the PNCNFs.

Physical Characterization. X-ray diffraction (XRD) measurements were conducted on a GBC MMA generator and diffractometer with Cu Kα radiation. Raman spectra were collected on a JOBIN YVON HR800 Confocal system with 632.8 nm diode laser excitation using a 300 lines mm^{-1} grating. Thermogravimetric analysis (TGA) was conducted on a SETARAM Thermogravimetric Analyzer (France). X-ray photoelectron spectroscopy (XPS) was performed on a VG Scientific ESCALAB 2201XL instrument using Al Kα X-ray radiation and fixed analyzer transmission mode. The XPS data were analyzed using CasaXPS software, and all the results were calibrated by C 1s = 284.6 eV. Field emission scanning electron microscope (FE-SEM) images were collected on a JEOL 7500 microscope, and transmission electron microscope (TEM) observations were carried out on a JEOL ARM-200F microscope. High-angle annular dark-field (HAADF) scanning transmission electron microscope (STEM) images and corresponding element mapping images were collected with the same TEM equipped with a Centurio SSD energy-dispersive X-ray spectroscopy (EDS) detector. Brunauer-Emmett-Teller (BET) surface area and pore size distribution (PSD) measurements were conducted by N_2 adsorption/desorption at 77 K on a Quantachrome Autosorb-IQ MP instrument.

Electrochemical Measurements. Rotating disk electrode (RDE) tests were conducted in a standard three-electrode cell connected to a computer-controlled potentiostat (Princeton 2273 and 616, Princeton Applied Research) at room temperature. A KCl saturated Ag/AgCl electrode and a platinum wire were used as the reference electrode and the counter electrode, respectively. The working electrodes were prepared by drop-pasting the samples onto a pre-polished glassy carbon (GC) electrode (5 mm in diameter). In brief, 4 mg catalyst was added into 2 mL Nafion®/H_2O/isopropanol (m/m/m = 0.05/10/50) solution and ultrasonicated for 30 min to form a homogeneous catalyst ink (2 mg/mL). A total of 30 μL catalyst ink was then pipetted onto the glassy carbon electrode surface and allowed to dry in a fume cupboard at room temperature for 30 minutes. For comparison, a commercially available Pt/C (20 wt.% Pt on Vulcan XC-72) electrode was also fabricated using the same method described above. To test the ORR performance, linear sweep voltammograms (LSVs) were collected in O_2 saturated 0.1 M KOH solution with different rotation speeds from 400 to 1600 rpm from 0.1 to -0.8 V with a scan rate of 10 mV s^{-1}. The kinetic analysis was performed on the basis of the Koutecky-Levich (K-L) equations:[1, 2]

$$\frac{1}{j} = \frac{1}{j_k} + \frac{1}{j_d} = \frac{1}{j_k} + \frac{1}{B\omega^{\frac{1}{2}}} \tag{1}$$

$$B = 0.2nF(D_{O_2})^{\frac{2}{3}}\nu^{\frac{-1}{6}}C_{O_2} \tag{2}$$

Where j, j_k, and j_d are the measured, kinetically controlled, and diffusion controlled current densities, respectively, and ω is the rotation rate, which is expressed in rpm. n represents the number of electrons transferred in the reduction of one O_2 molecule. F is the Faraday constant (F = 96485 C mol^{-1}), and D_{O2} is the diffusion coefficient of O_2 in 0.1 M KOH solution (D_{O2} = 1.9 × 10^{-5} cm^2 s^{-1}). ν is the kinematic viscosity of the 0.1 M KOH solution (ν = 0.01 cm^2 s^{-1}), and C_{O2} is the concentration of

O_2 in this solution (C_{O2} = 1 .2 × 10^{-6} mol cm^{-3}). The K-L plots were drawn based on $\omega^{-1/2}$ and j at a potential of -0.6 V in the limiting current potential region. From Equations (1) and (2), n and J_K (the kinetic-limiting current density) can be calculated from the slope of the linear fit line and the intercept of the K-L plots, respectively.[1, 3] The OER measurements were conducted in N_2 saturated 0.1 M KOH solution from 0.1 to 0.9 V at a scan rate of 10 mV s^{-1}. Cyclic voltammetry (CV) was performed in O_2 saturated 0.1 M KOH solution from 0.1 to -0.9 V at a scan rate of 10 mV s^{-1} and in Li-O_2 cells with the electrolyte consisting of 1 M lithium trifluoromethanesulfonate ($LiCF_3SO_3$) in tetraethylene glycol dimethyl ether (TEGDME).

For the preparation of the cathodes tested in Li-O_2 cells, 90 wt.% catalyst and 10 wt.% poly(tetrafluoroethylene) (PTFE) were mixed in isopropanol to make a catalyst slurry, which was homogeneously coated onto carbon paper and dried at 120 ^oC in a vacuum oven for 12 h. The substrate used as a gas diffusion layer was carbon paper (TGP-H-060, Toray) purchased from Fuel Cells Etc. The typical loading of the slurry for the cathode was about 1.0 ± 0.1 mg cm^{-2}. The CR 2032 coin-type cells with holes in their positive top covers were assembled in an Ar-filled Mbraun glove box (Germany) by stacking a glassy fiber separator between the catalyst cathode as the working electrode and the Li foil as the counter electrode. The electrolyte used in assembling the cell was 1 M $LiCF_3SO_3$ in TEGDME. Galvanostatic discharge/charge tests of the Li-O_2 cell were carried out at room temperature on a LAND CT 2001A multi-channel battery tester in an O_2-purged chamber with activated molecular sieves. The specific capacities were calculated based on the total amount of catalyst in the cathodes. To be specific, they are Pd, PNCNF, and Pd/PNCNF composites for the Pd, PNCNF, and composite cathodes, respectively.

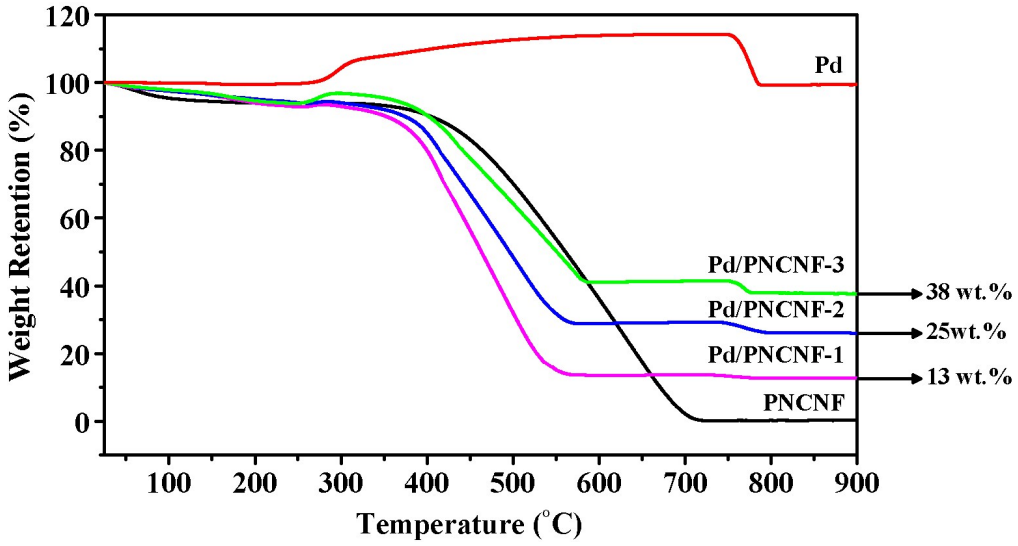

Fig. S1 TGA curves of the pure PNCNFs, the Pd/PNCNF composites, and the Pd particles.

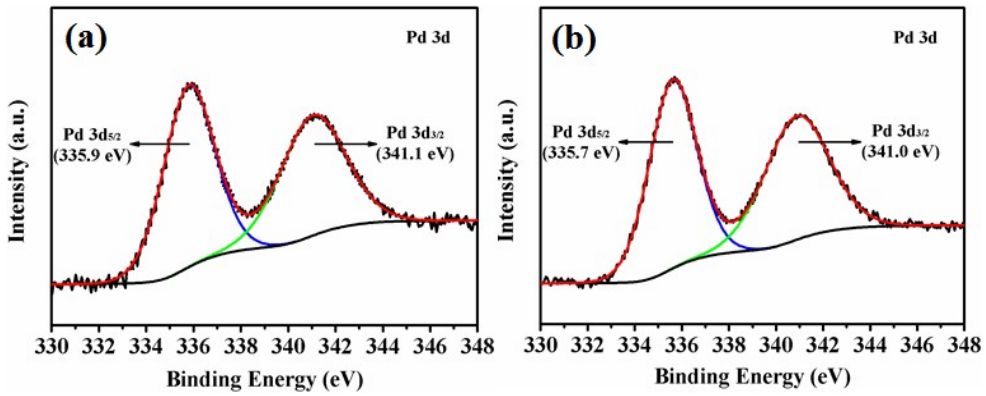

Fig. S2 High-resolution Pd 3d XPS spectra of (a) the Pd/PNCNF-1 and (b) the Pd/PNCNF-3 composites.

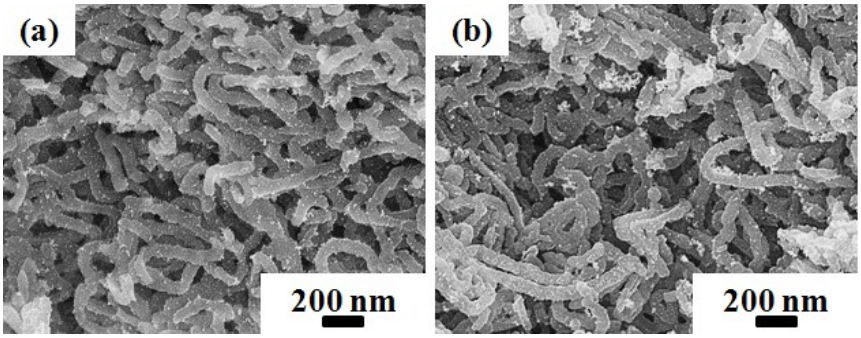

Fig. S3 FE-SEM images of (a) the Pd/PNCNF-1 and (b) the Pd/PNCNF-3 composites.

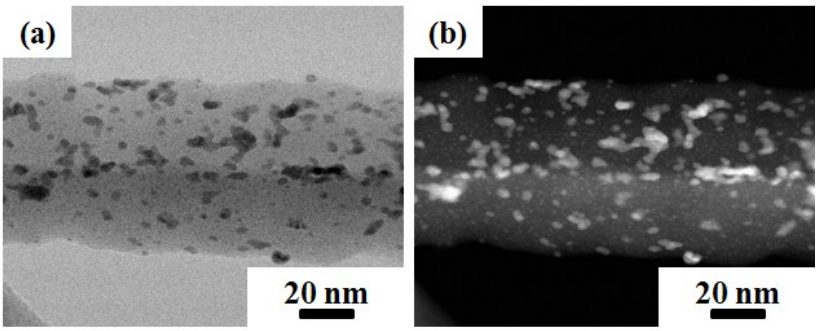

Fig. S4 (a) High resolution TEM and (b) corresponding scanning TEM (STEM) images of the Pd/PNCNF-3 composite.

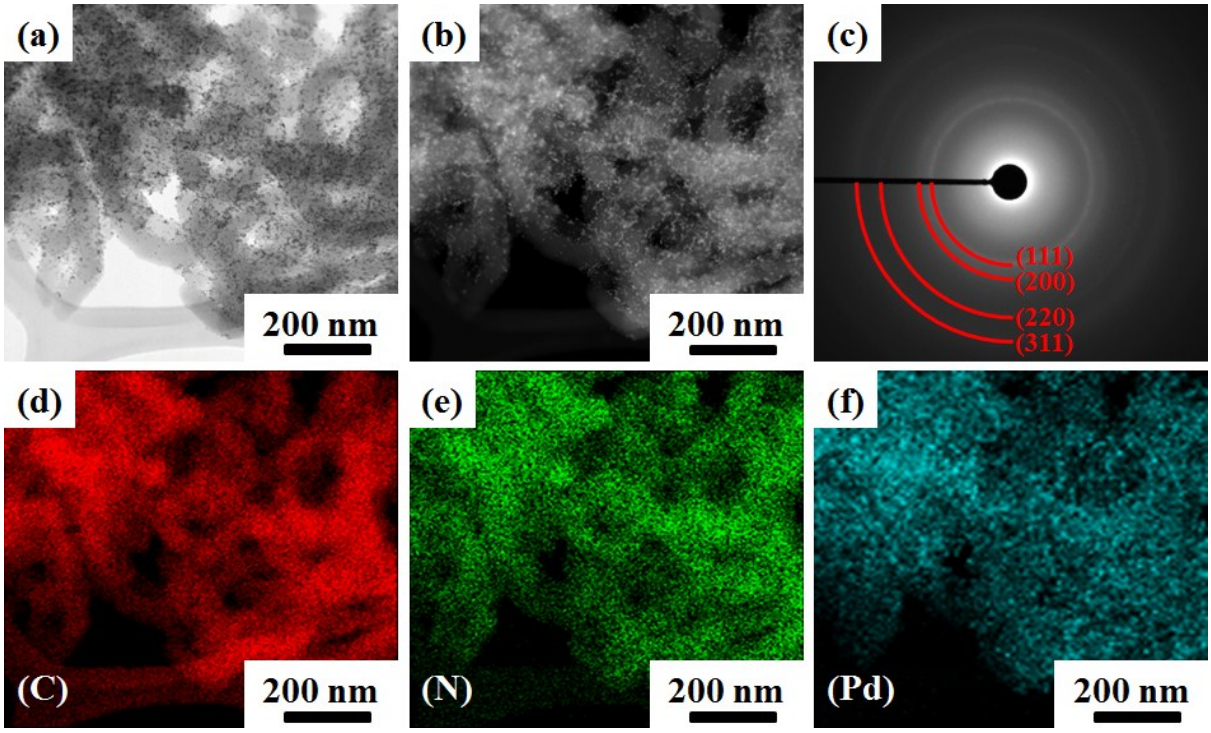

Fig. S5 (a) TEM and (b) scanning TEM (STEM) images, (c) associated SAED pattern, and (d)-(f) corresponding element mapping images of the Pd/PNCNF-2 composite.

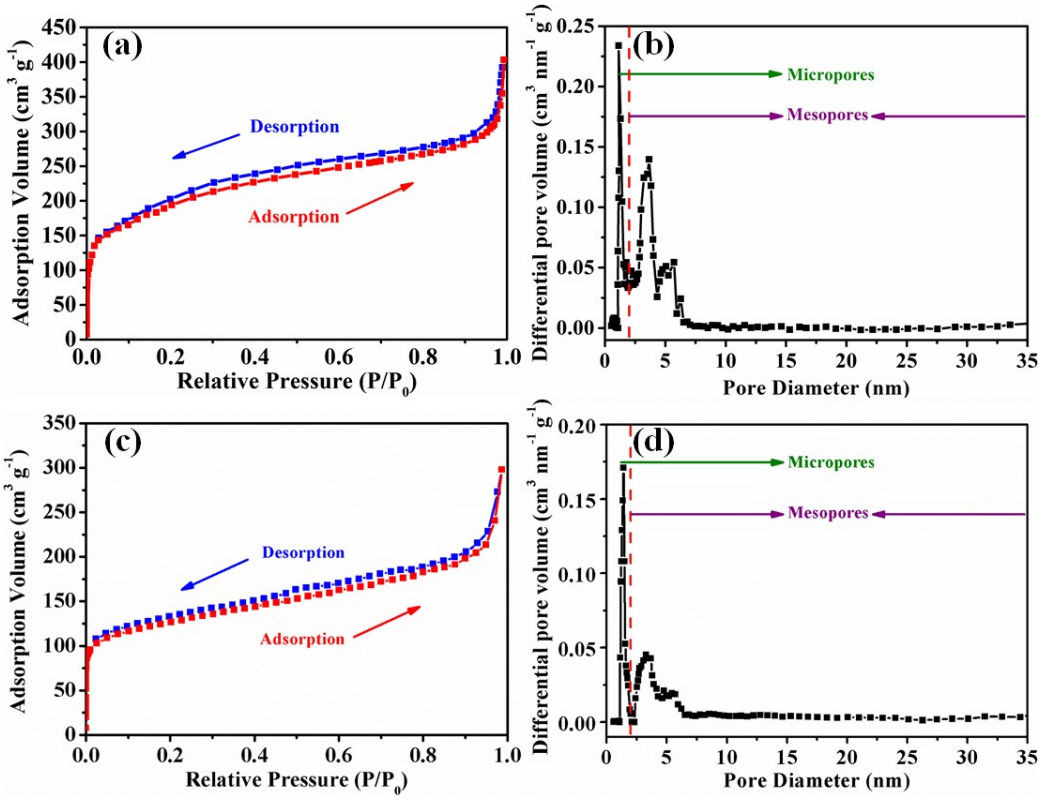

Fig. S6 N_2 adsorption-desorption isotherms (a, c), and (b, d) pore size distributions of (a, b) the PNCNFs and (c, d) the Pd/PNCNF-2 composite.

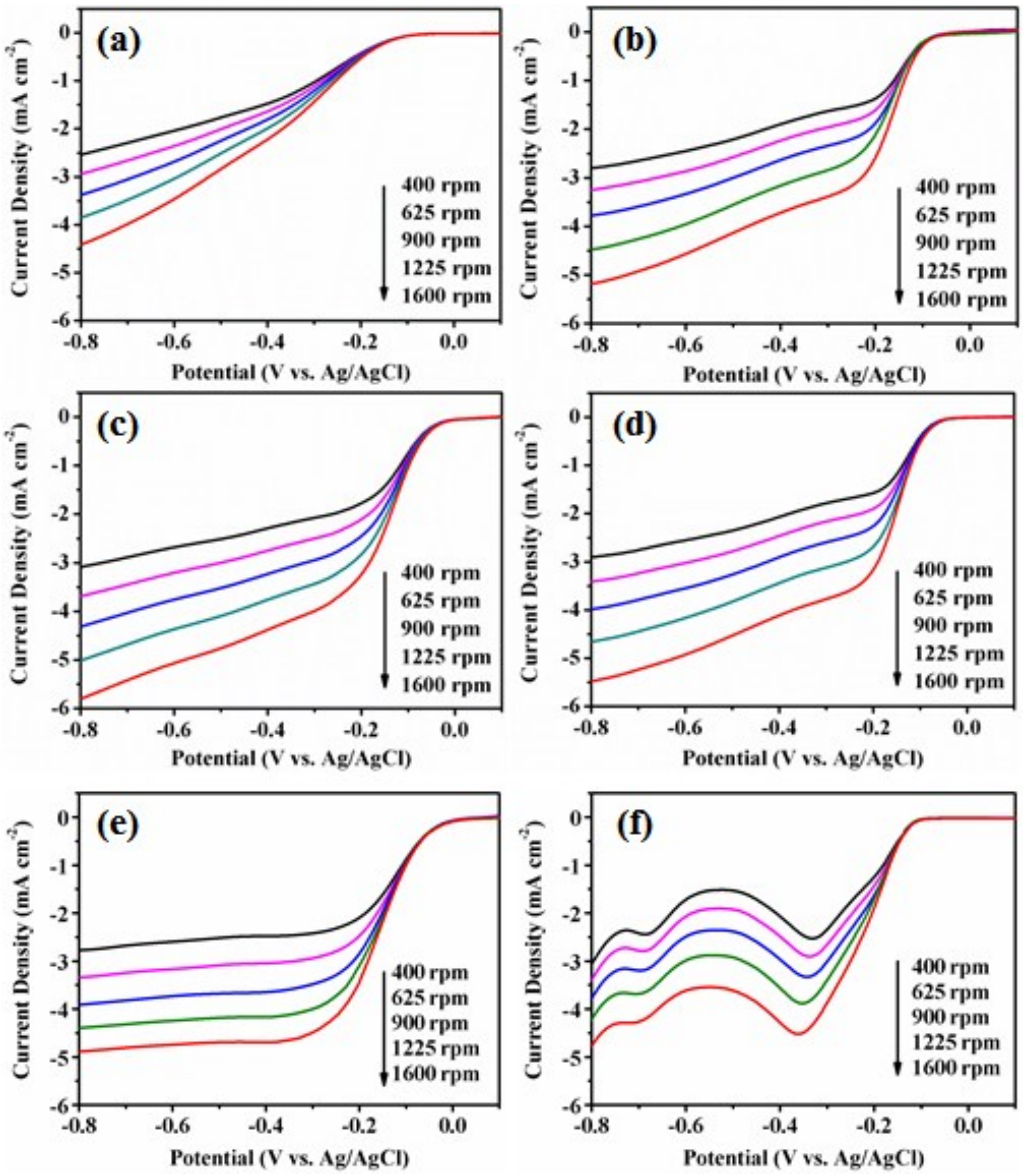

Fig. S7 ORR LSV profiles of (a) the pure PNCNFs, (b) the Pd/PNCNF-1 composite, (c) the Pd/PNCNF-2 composite, (d) the Pd/PNCNF-3 composite, (e) the commercial 20 wt.% Pt/C, and (f) the pure Pd at different rotation speeds.

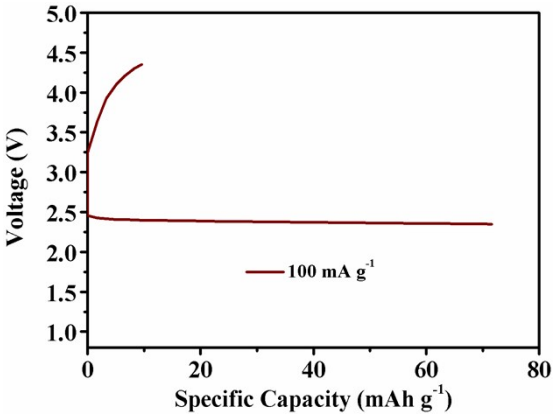

Fig. S8 Initial discharge/charge profiles of Li-O_2 battery containing carbon paper cathode from 2.35 to 4.35 V at 100 mA g^{-1}.

Table S1. Comparison of the Li-O_2 battery performance of Pd/PNCNF cathode with those of representative state-of-the-art cathodes reported in the literature.

Materials	Current Density/	1st Discharge Capacity[a]	Round-Trip Efficiency	Cycles/ Fixed Capacity	Ref.
Pd/PNCNF	100 mA g^{-1}	10080 mAh g^{-1}	~64%	50/1000 mAh g^{-1}	This work
Ketjen Black	100 mA g^{-1}	~6500 mAh g^{-1}	~63%	21/1000 mAh g^{-1}	4
Acetylene Black	100 mA g^{-1}	3234 mAh g^{-1}	~61%	23/1000 mAh g^{-1}	5
Super P	100 mA g^{-1}	~4000 mAh g^{-1}	~59%	26/1000 mAh g^{-1}	6, 7
Pd/CNT Sponge	0.1 mA cm^{-2}	~7000 mAh g^{-1}	~64%	16/1000 mAh g^{-1}	8
Pd/Carbon Nanoparticles	100 mA g^{-1}	~6600 mAh g^{-1}	~63%	-	9
Pd/Al_2O_3/Carbon Nanoparticles	100 mA g^{-1}	2750 mAh g^{-1}	~57%	11/1000 mAh g^{-1}	10
Pd/Co_3O_4 Nanoclusters	0.1 mA cm^{-2}	1843 mAh g^{-1}	~68%	70/300 mAh g^{-1}	11
Ru/Graphene Aerogels	0.1 mA cm^{-2}	~12000 mAh g^{-1}	~63%	50/500 mAh g^{-1}	12
Ru/CBC Nanofibers	200 mA g^{-1}	~2750 mAh g^{-1}	~68%	27/500 mAh g^{-1}	13
Pt/Graphene Nanosheets	100 mA g^{-1}	~3800 mAh g^{-1}	~63%	-	14
Pt/Carbon Nanotubes	160 mA g^{-1}	~2900 mAh g^{-1}	-	20/800 mAh g^{-1}	15
Au/Mn_3O_4 Nanowheats	100 mA g^{-1}	5759 mAh g^{-1}	~69%	60/1000 mAh g^{-1}	16
Au/Super P Nanoparticles	100 mA g^{-1}	-	-	31/500 mAh g^{-1}	17
Ag/MnO_2 Nanofibers	100 mA g^{-1}	4903 mAh g^{-1}	~68%	15/1000 mAh g^{-1}	18
Ag/Al_2O_3/Carbon Nanoparticles	100 mA g^{-1}	~3500 mAh g^{-1}	-	10/500 mAh g^{-1}	19
Co/PNCNF	100 mA g^{-1}	-	-	60/500 mAh g^{-1}	20

[a]The discharge capacities were calculated based on the amount of catalyst in the cathodes.

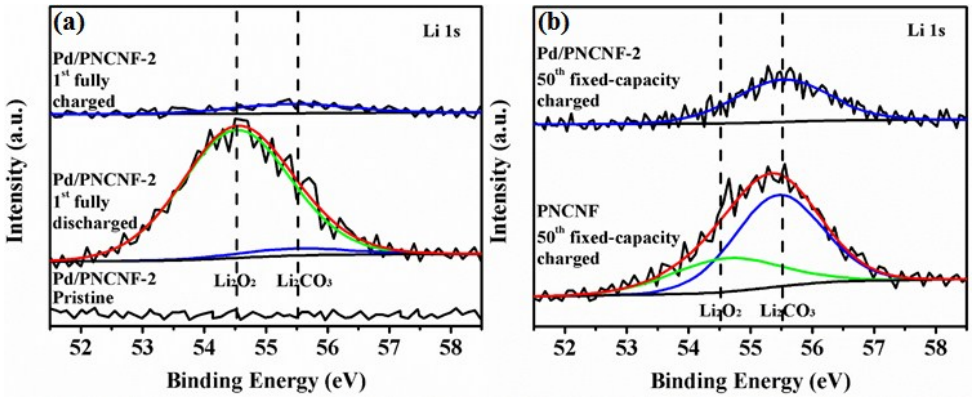

Fig. S9 High-resolution Li 1s XPS spectra of (a) the Pd/PNCNF-2 cathode before cycling, in the 1st cycle, when fully discharged (to 2.35 V), and in the 1st cycle, when fully charged (to 4.35 V), and (b) the PNCNF and the Pd/PNCNF-2 cathodes in the 50th cycle, after fixed-capacity charging.

References

1. J. T. Zhang, Z. H. Zhao, Z. H. Xia and L. M. Dai, *Nature Nanotechnology*, 2015, **10**, 444.
2. T. Sharifi, G. Hu, X. Jia and T. Wågberg, *ACS Nano*, 2012, **6**, 8904.
3. Y. Zhao, C. G. Hu, L. Song, L. X. Wang, G. Q. Shi, L. M. Dai and L. T. Qu, *Energy & Environmental Science*, 2014, **7**, 1913.
4. J. H. Kim, A. G. Kannan, H. S. Woo, D. G. Jin, W. Kim, K. Ryu and D. W. Kim, *J. Mater. Chem. A*, 2015, **3**, 18456.
5. L. Li, L. Shen, P. Nie, G. Pang, J. Wang, H. Li, S. Dong and X. Zhang, *J. Mater. Chem. A*, 2015, **3**, 24309.
6. S. Ma, L. Sun, L. Cong, X. Gao, C. Yao, X. Guo, L. Tai, P. Mei, Y. Zeng, H. Xie and R. Wang, *J. Phys. Chem. C*, 2013, **117**, 25890.
7. P. Li, J. Zhang, Q. Yu, J. Qiao, Z. Wang, D. Rooney, W. Sun and K. Sun, *Electrochimica Acta*, 2015, **165**, 78.
8. Y. Shen, D. Sun, L. Yu, W. Zhang, Y. Shang, H. Tang, J. Wu, A. Cao and Y. Huang, *Carbon*, 2013, **62**, 288.
9. Y. Lei, J. Lu, X. Y. Luo, T. P. Wu, P. Du, X. Y. Zhang, Y. Ren, J. G. Wen, D. J. Miller, J. T. Miller, Y. K. Sun, J. W. Elam and K. Amine, *Nano Lett.*, 2013, **13**, 4182.
10. J. Lu, Y. Lei, K. C. Lau, X. Luo, P. Du, J. Wen, R. S. Assary, U. Das, D. J. Miller, J. W. Elam, H. M. Albishri, D. A. El-Hady, Y. K. Sun, L. A. Curtiss and K. Amine, *Nat. Commun.*, 2013, **4**, 2383.
11. L. Leng, X. Zeng, H. Song, T. Shu, H. Wang and S. Liao, *J. Mater. Chem. A*, 2015, **3**, 15626.
12. J. Jiang, P. He, S. Tong, M. Zheng, Z. Lin, X. Zhang, Y. Shi and H. Zhou, *NPG Asia Mater*, 2016, **8**, e239.
13. S. Tong, M. Zheng, Y. Lu, Z. Lin, X. Zhang, P. He and H. Zhou, *Chemical Communications*, 2015, **51**, 7302.
14. Y. Yang, M. Shi, Q. F. Zhou, Y. S. Li and Z. W. Fu, *Electrochem. Commun.*, 2012, **20**, 11.
15. J. Li, Y. Zhao, M. Zou, C. Wu, Z. Huang and L. Guan, *ACS Appl. Mater. Interfaces*, 2014, **6**, 12479.
16. J. Qu, M. Lu, C. Xu, B. Ding, Y. Zhan, J. Yang and J. Y. Lee, *Nanoscale*, 2014, **6**, 12324.
17. P. Balasubramanian, M. Marinaro, S. Theil, M. Wohlfahrt-Mehrens and L. Jörissen, *J. Power Sources*, 2015, **278**, 156.
18. M. Lu, J. Qu, Q. Yao, C. Xu, Y. Zhan, J. Xie and J. Y. Lee, *ACS Applied Materials & Interfaces*, 2015, **7**, 5488.
19. J. Lu, L. Cheng, K. C. Lau, E. Tyo, X. Y. Luo, J. G. Wen, D. Miller, R. S. Assary, H. H. Wang, P. Redfern, H. M. Wu, J. B. Park, Y. K. Sun, S. Vajda, K. Amine and L. A. Curtiss, *Nat. Commun.*, 2014, **5**, 4895.
20. Y. J. Kim, H. Lee, D. J. Lee, J. K. Park and H. T. Kim, *ChemSusChem*, 2015, **8**, 2496.